Environmental Science and Pollution Research (2020) 27:3756–3767
https://doi.org/10.1007/s11356-019-05794-8

MULTI-STRESSORS IN FRESHWATER AND TRANSITIONAL ENVIRONMENTS: FROM LEGACY POLLUTANTS TO EMERGING ONES

Radiolabeling of amide functionalized multi-walled carbon nanotubes for bioaccumulation study in fish bone using whole-body autoradiography

Youssouf Djibril Soubaneh[1] · Emilien Pelletier[2] · Isabelle Desbiens[2] · Claude Rouleau[2]

Received: 29 June 2018 / Accepted: 19 June 2019 / Published online: 12 July 2019

Abstract

Commercial and medicinal applications of functionalized carbon nanotubes (f-CNTs) such as amidated f-CNTs are expanding rapidly with a potential risk exposure to living organisms. The effects of amidated f-CNTs on aquatic species have received a limited attention. In this work, an easy wet method to prepare [^{14}C]-label amide multi-walled carbon nanotubes (MWNTs) is reported. Labeled carbon nanotubes were prepared by successive reactions of carboxylation, chloroacylation, and final amidation using [^{14}C]-labeled ethanolamine. The f-CNTs were characterized using elemental analysis, electron dispersive X-ray, transmission electron microscopy, thermogravimetric analysis, and Raman and FTIR spectroscopy. An uptake experiment was carried out with juvenile Arctic char (*Salvelinus alpinus*) using water dispersed amidated [^{14}C]-f-CNTs to assess their biodistribution in fish tissues using whole body autoradiography. The radioactivity pattern observed in fish head suggests that f-CNTs were accumulated in head bone canals, possibly involving an interaction with mineral or organic phases of bones such as calcium and collagen. This f-CNTs distribution illustrates how important is to consider the surface charges of functionalized carbon nanotubes in ecotoxicological studies.

Keywords Carbon nanotubes · Amide functionalization · Radiolabeling method · Fish · Canal bones

Introduction

First discovered in early 1990s (Iijima 1991), two classes of carbon nanotubes (CNTs) are now commercially available as single-walled carbon nanotubes (SWNTs) and multi-walled carbon nanotubes (MWNTs). The lack of solubility of unfunctionalized CNTs in all organic solvents and water (Tasi et al. 2006) severely limited their use in monodisperse solutions and constrained the investigation of their potential effects on aquatic environment. Chemical techniques to modify CNT surface are progressing rapidly and examples of surface functionalization of nanotubes and their applications to bone tissue engineering or biomedical applications have been published in recent years (Saffar et al. 2009; Bacakova et al. 2014; Sajid et al. 2016). The number and diversity of products and technologies containing CNTs, particularly functionalized carbon nanotubes (f-CNTs), continue to rise at an accelerated rate (Karimi et al. 2015; Jacoby 2015**).** Functional groups, such as ethanolamine (EA), are associated with functionalized CNTs. The amidated CNTs (**CNT-A)** are used for their antimicrobial activity, drug carrier capacity in biomedicine and as an alternative to the heavy metal nanoparticles (NPs) (Wijnhoven et al. 2009; Zhang et al. 2011; Zardini et al. 2014).

Functionalized CNTs (f-CNTs) have a large number of active binding sites on their surface. Thus, their dispersibility in water, their interaction with particulate matter of aquatic system, and their impacts on biological matrix can be enhanced compared to raw CNTs (Cui et al. 2010; Petersen et al. 2011).

Responsible editor: Philippe Garrigues

✉ Youssouf Djibril Soubaneh
Youssoufdjibril_Soubaneh@uqar.ca

[1] Département de biologie, chimie et géographie, Université du Québec à Rimouski, 300, Allée des Ursulines, Rimouski, QC G5L 3A1, Canada

[2] Institut des sciences de la mer de Rimouski, Université du Québec à Rimouski, 310 Allée des Ursulines, Rimouski, QC G5L 3A1, Canada

The CNT interactions with pesticides, such as carbofuran, enhance the ecotoxic effects of these compounds on fish by increasing transfer through cellular membrane (Campos-Garcia et al. 2016). Furthermore, surface charge interactions of f-CNTs with lead (Pb) affect this bioavailability for zooplankton (Jang and Hwang 2018). Moreover, it was shown that CNT toxicity on guinea pigs is greater compared to other nanomaterials such as fullerenes (Jia et al. 2005). Using functionalized CNTs, with both hydrophilic/hydrophobic properties, is appropriate to a better understanding of CNT behavior in aquatic environment. Taurine, with a solubility in water of 50 mg mL^{-1} at 20 °C, has been proposed in the functionalization of CNTs for studying the fate of nanotubes in mice (Deng et al. 2007). However, drawbacks, at odds with green chemistry, were reported in the synthesis process of taurine from ethanolamine (Widiyarti et al. 2009) which involves esterification and sulphonation reactions. Sulphonation has a long reaction time at high temperature; the purification is difficult and the yield of separated products is low. Ethanolamine (EA), with higher solubility in water (100 mg mL^{-1} at 20 °C), fewer synthetic steps, and easier purification process, may be more suitable for CNT functionalization and particularly for [^{14}C]-labeling (Riddick et al. 1986).

Only a few raw or carboxylated CNTs bioaccumulation results have been reported for fish and aquatic invertebrates (Bjorkland et al. 2017) due to the limited number of analytical methods available to detect and quantify CNTs in biological samples (Maes et al. 2014). The few studies reporting the impacts of CNTs on fish mainly targeted organs such as the gills, gut, liver, and brain (Jackson et al. 2013; Maes et al. 2014; Sohn et al. 2015). The use of radioactive isotopes as a tool to locate nanoparticles by autoradiography method has only been developed recently (Solon 2007), but has already proven to be a promising approach to locate and quantify metal nanoparticles in whole-body aquatic organisms (Al-Sid-Cheikh et al. 2011).

Radiolabeled f-CNTs are useful materials in studying and understanding their impacts on different geochemical and biological matrices of environment (Petersen et al. 2011; Zhang et al. 2012; Maes et al. 2014). Catalytic vapor deposition (CVD) or wet chemistry approaches can be used for CNT [^{14}C]-labeling. For CVD process, labeled nanotubes have been prepared by introducing [^{14}C]-methane, as a carbon source, within the synthesis of raw [^{14}C]-CNTs (Chen et al. 1997). This technique, recently adapted for aquatic organisms applications (Petersen et al. 2009; Maes et al. 2014), requires the implementation of specialized materials and methods, such as electric-arc technique, usually utilized for the production of raw CNTs (Hou et al. 2001). The preparation of labeled CNTs by grafting labeled functional groups on raw CNTs using a wet chemistry approach has received limited attention. To our knowledge, only two [^{14}C]-labeling strategies of CNTs have been reported. Georgin et al. (2009) proposed a labeling method for MWNTs using Cu and Pd as catalysts in their process. Deng et al. (2007) reported a MWNTs labeling strategy using taurine as a functional group. This latter strategy is suitable for studying the fate of functionalized CNTs in the environment by using ethanolamine as a functional group bearing amine and alcohol functionalities which improve their interaction capacities with aquatic environmental matrices (such as sediments and/or organisms).

Up to now, the raw distribution of CNTs on bony structures of fish was rarely investigated, and the impact of amide functionalized CNTs was not investigated in aquatics species (Bjorkland et al. 2017). Our first objective in this work was to detail a modification method of small and large raw MWNTs by carboxylation and grafting [^{14}C]-ethanolamine. All carboxylated and amidated CNTs were characterized to evaluate their surface chemical transformation during functionalization. Our second objective was to describe, for the first time, the whole body autoradiographic results of an in vivo experiment where juvenile Arctic char (*Salvelinus alpinus*) was exposed to amidated [^{14}C]-f-CNTs for a short time in an attempt to locate main accumulation sites of carbon nanotubes highly dispersed in water. It was not intended to observe toxic effects.

Materials and methods

Chemicals and equipment

The large multi-walled CNTs (CNT1; outer diameter 110–170 nm; length 5–09 μm; purity > 90%) were obtained from Sigma-Aldrich Canada. The small multi-walled CNTs (CNT2; outer diameter 30–50 nm; length 10–20 μm; purity > 95%) were purchased from Cheap Tubes, inc. (USA). Nitric acid (70%), sulphuric acid (98%), and acetone were provided by Fisher Scientific Canada. Thionyl chloride, ethanolamine (95.5%), and tricaine methanesulfonate (MS-222) were purchased from Sigma-Aldrich Canada. Radiolabeled [^{14}C]-ethanolamine, with a specific activity of 2.11 GBq $mmol^{-1}$ was obtained from Moravek radiochemicals (USA).

The CHNO elemental analysis of CNTs was performed with both Perkin Elmer 2400 (USA) and Carlo Erba 1108 (Italy) analyzers. The surface analysis of CNT1 and CNT2 was carried out by electron dispersive X-ray spectroscopy (EDX) (INCA microanalyzer, Oxford Scientific, USA). The thermogravimetric spectra were recorded with a 6200 TG/DTA instrument (Seiko, Japan). The Raman spectra were performed on LabRam HR800 spectrometer (Horiba, Japan). The Fourier transform infrared spectra (FTIR) were recorded with a FTIR/FTNIR (Perkin Elmer, USA) with a resolution of 4 cm^{-1} at 32 scans on KBr pellets. Transmission electron microscopy (TEM) images were captured using a LVEM 5 (Delong America, USA). [^{14}C]-labeled nanotubes were

burned at 800 °C for 2 min under a stream of oxygen gas in a model A-307 sample oxidizer (Perkin Elmer, USA), and the [$^{14}CO_2$] released during the combustion process was captured in [^{14}C]-scintillation cocktail (Insta-GelPlus). The radioactivity in the mixture was measured using a Tri-Carb 2800 liquid scintillation counter (Perkin Elmer, USA). For calibration and evaluation of the sample oxidizer recovery, a duplicate standard was made by uniformly inoculating raw CNTs with 100 Bq of labeled ethanolamine.

Preparation of [^{14}C]-labeled CNTs

Raw CNTs (CNT1 and CNT2) were functionalised following the Deng et al. (2007) method with some modifications and using [^{14}C]-labeled ethanolamine. The scheme of the proposed transformation of CNTs is given by the following equation where $^{(*)}$ stands for labeled [^{14}C]:

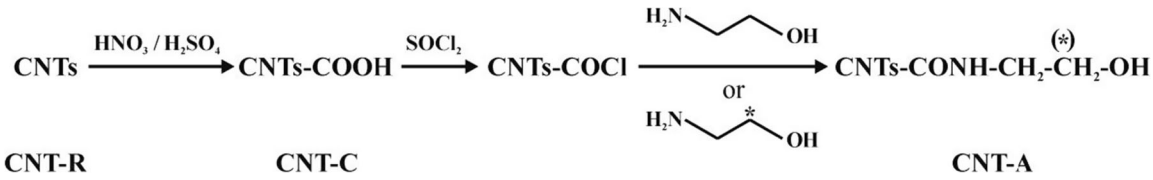

In the first step, 100 mg of commercial CNTs were loaded in a round-bottom flask and 7 mL of a 3:1 (by volume) mixture of concentrated sulphuric and nitric acids were added to oxidize raw CNTs. The mixture was stirred at 80 °C during 90 min, then diluted with 100 mL of deionised water, and filtered on 0.2-μm GHP (polypropylene) filter. The residual black solid was washed with deionised water until the pH of filtered water was neutral. The solid was then dried in vacuum at 60 °C overnight to yield CNT-COOH, identified hereafter as CNT1-C and CNT2-C for large and small CNTs, respectively. The dry solid was placed in a round-bottom flask, dispersed in 6 mL of $SOCl_2$ by ultrasonication for 1 h (Branson 5210 ultrasonic bath) and then refluxed under a nitrogen atmosphere for 24 h. The unreacted $SOCl_2$ was removed by low pressure evaporation to yield chloroacylated CNTs. Finally, the round-bottom flask was immerged in cold water; 6 mL of ethanolamine (EA) was added dropwise, and the solution was stirred at room temperature for 24 h. At the end of the reaction, 50 mL of acetone was added to the mixture to precipitate functionalized nanotubes, which were collected by filtration on 0.2-μm GHP filter. This solid was dispersed in 100 mL of anhydrous ethanol to eliminate remaining ethanolamine, filtered, and then vacuum dried to yield the amidated CNT-CONH-ETOH product, identified as CNT1-A and CNT2-A for large and small CNTs, respectively.

The [^{14}C]-labeled f-CNTs were prepared using synthesis protocol similar to unlabeled f-CNTs above, by adding [^{14}C]-ethanolamine ([^{14}C]-EA) to the chloroacylated CNTs in the last step for the protocol. An aliquot of [^{14}C]-EA was added to 6 mL of not labeled EA to obtain a final activity of about 100 Bq mL^{-1}. At the end of the reaction, the mixture was treated as described above and the [^{14}C]-labeled CNT1-A and CNT2-A were washed successively with large volumes of anhydrous ethanol and diethyl ether to eliminate any traces of unreacted [^{14}C]-ethanolamine. Bulk radioactivity was determined by liquid scintillation after oxidation to [$^{14}CO_2$].

Exposure of fish to radiolabeled CNTs

Juveniles Arctic char (*Salvelinus alpinus*) (weight 25–27 g) were grown under laboratory conditions at the Institut des Sciences de la Mer de Rimouski (UQAR/ISMER, Qc, Canada) and held in dechlorinated running freshwater. One week of acclimation was respected prior experiment by keeping all fish in 30-L aquarium with running freshwater (8–10 °C) under 12–12 h light-dark cycle and fed daily with commercial pellets (Nutrafin cichlid pellets). To perform this work, an ethical approval was obtained from the Animal Care Committee of our university (CPA-44-11-95).

^{14}C-labeled CNT1 and CNT2 were dispersed by sonication for 3 min in cold water (1 °C) to minimize damage to the nanotubes. It has been previously shown that CNTs sonication in an ice-water bath reduces CNTs damage (Heller et al. 2005). One fish was exposed to each type of CNT. The fish were transferred separately in two 5-L containers and exposed to [^{14}C]-CNTs for 3 h in filtered (0.2 μm GHP filter) freshwater containing a final concentration of 90 mg L^{-1} for CNT2, and 160 mg L^{-1} for CNT1. These concentrations are above the environmental concentration, but in the range of those (from 0.1 to 240 mg.L^{-1}) used for the studies of CNT toxicity on aquatic organisms (Jackson et al. 2013). We used relatively high f-CNTs concentrations to allow detection of the f-CNTs distribution by autoradiography. Indeed, the CNT1/CNT2 radioactivity is approximately four orders of magnitude lower than those usually used in uptake studies (e.g., 0.45 MBq mg^{-1} in Georgin et al. (2009)). Otherwise, the weak radioactivity used in this work shows the high sensibility of the whole

body autoradiography technique. As the objective of the work was to locate the distribution of carbon nanotubes on the whole body of the fish over a short exposure time, no toxicity biotest was conducted. To investigate a possible artifact from free labeled ethanolamine, one juvenile fish was exposed (20 h) to a mixture of radiolabeled [^{14}C]-ethanolamine and not labeled ethanolamine with a total radioactivity of 410 Bq L^{-1}. To maximize a possible interaction between free ethanolamine and the bone system and be able to detect it by autoradiography, a longer exposure time than that of f-CNTs has been used.

Biodistribution by whole body autoradiography

At the end of the exposure time, fish were euthanized by immersion in 100 mg mL^{-1} tricaine methanesulfonate for 10 min. Fish were embedded in a 5% carboxymethylcellulose gel and frozen in liquid nitrogen. The resulting polymer block was sliced at −25 °C with a cryo-microtome (Leica CM3600). A series of 50-μm thick tissue sections ($n = 42$, total sections per fish) were collected every 0.75 mm, freeze-dried for 48 h, and exposed 1 week on phosphor screens (Biotech, UK) for 500 h. Digital scans of the phosphor screens were obtained with a cyclone storage phosphor system (Perkin Elmer, USA). The biodistribution of the [^{14}C]-labeled CNTs in fish whole body was visualized with Optiquant software (Optiquant v 5, Perkin Elmer).

Results and discussion

Functionalization, characterization, and radiolabeling of CNTs

Carboxylated and amidated CNT products (f-CNT) derived from CNT1 or CNT2 were much easier to disperse in water compared to raw CNTs as expected from previous papers reporting on functionalization of carbon nanotubes (Georgin et al. 2009; Mananghaya 2015). In addition, small f-CNT2 nanotubes were more dispersible than larger ones. After sonication for 1 min or less to avoid breakdown of nanotubes, both water suspensions of f-CNT1 and f-CNT2 were stable for weeks without visible aggregation and sedimentation. To assess the level of derivatization of the nanotubes and get a better understanding of the behavior of these functionalized nanotubes in water, a chemical characterization of carboxylated and amidated CNT1 and CNT2 was conducted. The characterization of f-CNTs was performed using non radioactive samples assuming [^{14}C]-CNTs exhibited same physical and chemical properties.

The size of raw CNTs indicated by the suppliers was confirmed by TEM showing short and long nanotubes, approximately between 1 and 10 μm. Outer diameters of CNT1-R and CNT2-R ranged from 90 to 180 nm and from 20 to 60 nm, respectively**.** TEM images are shown for raw, carboxylated, and amidated CNT1/CNT2 (Fig. 1 and Figure S1**).** The level of –COOH substitution at surface of nanotubes is a function of reaction time and temperature (Forest and Alexander 2007).

The elemental analysis (CHNO) of the raw and derivatized CNTs (Table 1) provided useful information on the success of functionalization strategy. The results of the composition analysis showed that a relatively important amount of oxygen, from 11.8 to 13.82% by mass, was introduced in the raw CNTs after carboxylation reaction. These results confirm the presence of carboxyl and/or hydroxyl functionalities in the CNT-C derivatives. The amidation process inserted between 2.68 and 5.07% N (by mass) into CNT-A, suggesting that only a portion of the carboxyl groups were amidated. However, about two times more nitrogen was introduced in CNT2 compared to CNT1. Results also showed an enhancement of hydrogen (H) content, from 0.17 to 1.26% for CNT1 and 0.13 to 2.63% for CNT2, in derivatized CNTs corresponding to the introduction of oxygen-containing functional groups on CNT surface, such as carboxyl (–COOH) and amide (–NH–ETOH) groups.

Results obtained with elemental analysis were corroborated by surface composition analysis using electron dispersive X-ray (EDX) (Table 1). The EDX on the sample treated with nitric/sulphuric acid (CNT-C) showed the presence of about 12.6 to 12.8 % O. In addition, we found traces of sulphur (0.2–1.35%) attributed to the presence of unreacted sulphonic groups (–SO_3H). Finally, EDX analysis showed the presence of nickel (0.45%) in the raw CNT2, originating from the catalyst precursor used in synthesis of raw nanotubes, which was removed after oxidation process with nitric/sulphuric solution to obtain CNT2-C.

The thermogravimetric analysis of raw and carboxylated CNTs was carried out to get a better understanding of their structures. Different structural forms of the CNTs can reflect different oxidation behavior as a function of the chemical groups grafted on CNT surfaces. For example, disordered carbon of derivate CNTs could be oxidized around 500 °C because of their lower activation energy for the oxidation (Hou et al. 2001). The TG (thermogravimetry) and DTG (derivative thermogravimetry) curves of the raw and carboxylated CNT1 and CNT2 compounds are illustrated in Fig. 2. No weight loss is observed for the raw CNTs during the heating process, but losses during the thermal degradation of CNT1-C and 2-C indicated a multi-stage process. A first loss of 2.11% by weight is detected for the CNT1-C at temperature of 150 °C (Fig. 2a) and is assigned to evaporation of the absorbed water and small remaining nitric acid as suggested by the presence of nitrogen element in CNT-C (Table 1). The stepwise losses observed from 150 to 350 °C represent about 5.85% by weight and are attributed to the decarboxylation of the carboxylic groups. Finally, the thermal degradation of CNT1-C above

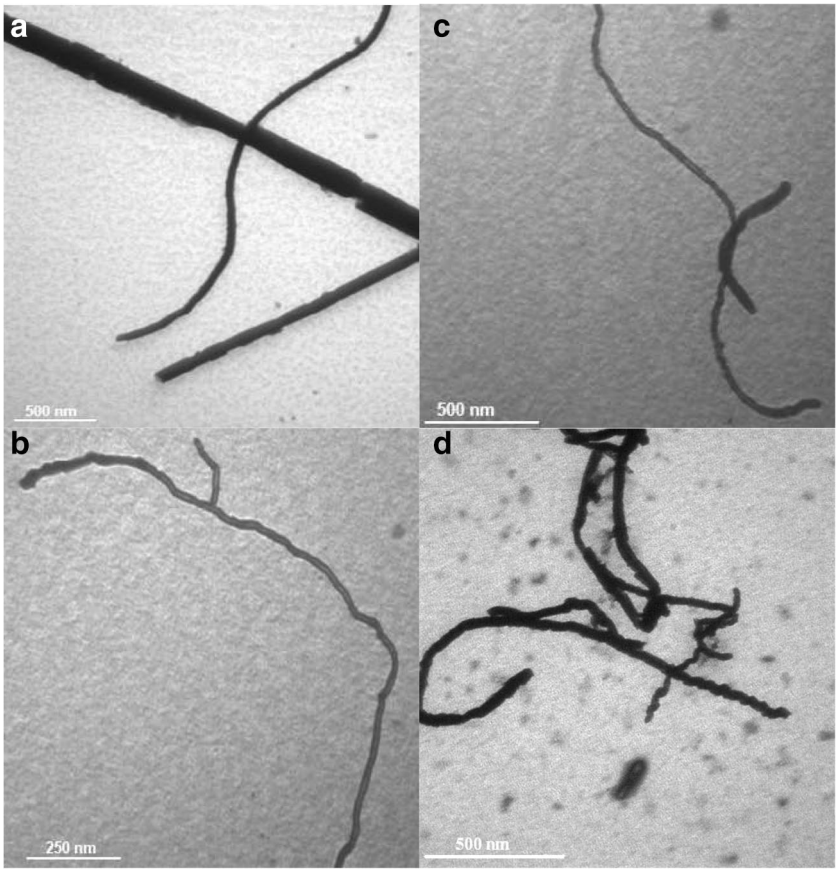

Fig. 1 TEM images illustrating some carbon nanotubes used in this experiment. **a** carboxylated CNT1. **b** Raw (native) CNT2, **c** Carboxylated CNT2. **d** amidated CNT2

350 °C showed weight loss of 5.91%. This loss can be mainly explained by the oxidation of the disordered carbon or the elimination of hydroxyl functionalities attached to the CNTs (Grandi et al. 2006). Overall, weight losses observed for the CNT2-C (Fig. 2b) are more important than those of CNT1-C, and the difference is attributed to a higher carboxylated level of CNT2-C (Table 1).

The Raman spectroscopy analysis showed three characteristic bands (Kaempgen et al. 2008) named the D-band at ~ 1350 cm^{-1}, G-band at ~ 1570 cm^{-1}, and D'-band at ~ 2700 cm^{-1} as illustrated in Fig. 3 and Figure S2 for the CNT1 and CNT2. D-band is observed after oxidation (carboxyl or hydroxyl groups) of CNTs and is proportional to the oxidation level of CNTs. The D-band is attributed to the defect in the carbon nanotubes and related to the presence of disordered or amorphous carbon in CNTs (Datsyuk et al. 2008). The ratio between intensities of D-band (I_D) and G-band (I_G) increase when nanotubes are oxidized (Kaempgen et al. 2008). The I_D/I_G of the CNT1-C and CNT2-C are 0.45 and 0.80, respectively (Table 1). This is mainly attributed to the insertion of carboxyl and hydroxyl functions at sp3-defects in the CNTs as reported for oxidized CNTs (Kaempgen et al. 2008; Datsyuk et al. 2008). The I_D/I_G ratio observed for CNT2-C (Fi.ure S2) suggests a high carboxylation of CNT2-C since the oxygen

Table 1 Elemental composition, EDX, and Raman analysis of carbon nanotubes. CNT1-R and CNT2-R are large and small raw nanotubes as received. CNT1-C and CNT2-C are nanotubes after carboxylation, and CNT1-A and CNT2-A are nanotubes after amidation

Sample	Elemental composition				EDX analysis				Raman
	% C	% H	% N	% O	%C	%O	%S	%Ni	I_D/I_G
CNT1-R	99.43	0.17	0.0	0.0	99.33	0.67	n.d.[a]	n.d.	0.19
CNT1-C	86.05	0.44	0.19	11.82	86.13	12.86	1.1	n.d.	0.45
CNT1-A	82.63	1.26	2.68	11.82	81.64	13.6	1.35	n.d.	n.a.[b]
CNT2-R	97.64	0.13	0.00	0.21	99.54	0.46	n.d.	0.45	0.61
CNT2-C	83.17	0.61	0.12	13.82	86.74	12.64	0.20	n.d.	0.80
CNT2-A	66.46	2.63	5.07	22.70	64.13	23.90	n.d.	n.d	n.a

[a] Not detected; [b] Not available

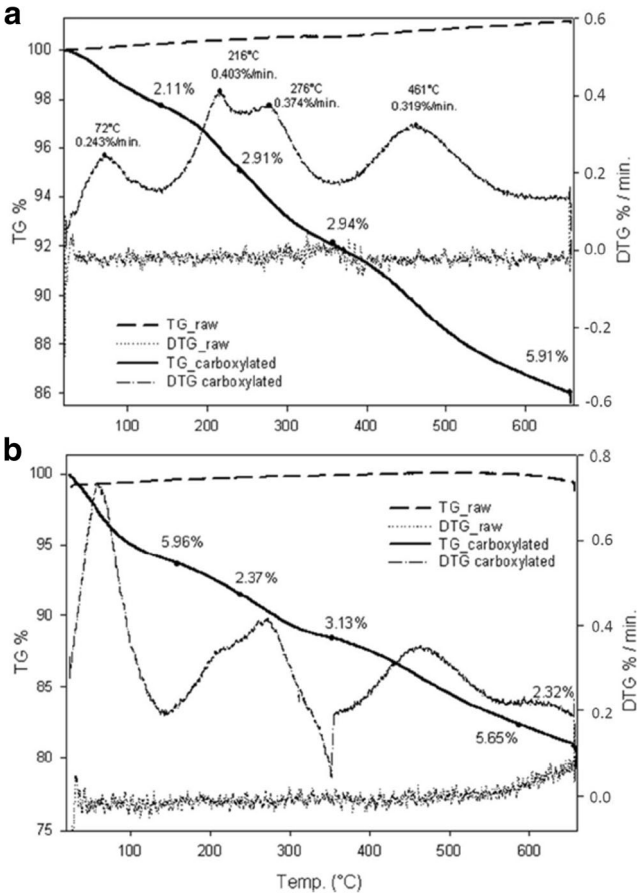

Fig. 2 Thermogravimetric (TG) and derivative thermogravimetric (DTG) curves of **a** raw and carboxylated CNT1 as a function of the temperature and **b** raw and carboxylated CNT2 as a function of the temperature

groups, available in CNT2-R (Table 1), could stimulate the insertion of –COOH groups during carboxylation process.

FTIR transmission spectra of raw and modified CNT1 and CNT2 are given in Fig. 4 and Figure S5. These spectra confirm the oxidation of sp2 carbon of raw CNT-R to sp3 hybridized and the existence of C = O and OH functional groups. For instance, CNT1 FTIR spectra show the appearance of amide bands being a characteristic of covalently bonded amide. The band at 1720 cm^{-1} is attributed to C = O stretching of the carboxyl acid. The bands at 1385 and 3435 cm^{-1} are assigned to OH stretching (Wu and Liano 2007). The presence of these bands correlate well with the O content in CNT-C compared to CNT-raw without oxidation (Table 1).

All IR spectra showed a small band at 1575 cm^{-1} resulting from stretching vibration of isolated C = C of the aromatic structure of nanotubes (Martinez et al. 2003).The C = O stretching frequencies of the amide bond formed by the functionalization reaction appear at 1640 cm^{-1}. The bands observed at 1115 and 1195 cm^{-1} can be attributed to the–OH stretching of the alcohol function of ethanolamine. Finally, the N–H stretching (at 3435 cm^{-1}) is overlapped by the large –OH stretching at the same frequency.

The bulk radioactivity of [^{14}C]-labeled CNT1 and CNT2 was 2.5 and 4.6 Bq mg^{-1}, respectively. The CNT2 radioactivity was twice the one of CNT1 due to a better amidation of CNT2-A compared to CNT1-A as shown in Table 1. Thus, more [^{14}C]-labeled EA molecules were inserted in the CNT2-A structure. This specific radioactivity is very lower than those reported in others labeling strategies (e.g., 0.45 MBq mg^{-1}; Georgin et al. 2009). To improve the bulk radioactivity of labeled CNTs and get closer to environmental concentrations, a double [^{14}C]-labeled diethanolamine or isopropanolamine can be used with a smaller reaction volume. Moreover, the yield and time of the reaction should be improved in the future to avoid a possible destruction of CNTs during carboxylation process ([^{14}C]-labeling).

Radioactivity pattern

The analysis of autoradiograms showed a radioactivity pattern located mainly in the head of Arctic char exposed to f-CNTs. Figure 5 illustrates different tissue sections of the Arctic char head exposed to [^{14}C]-CNT2-A (Fig. 5a, b) and [^{14}C]-CNT1-A (Fig. 5c, d). The radioactivity pattern suggests that the amidated f-CNTs distribution follows some particular lines located in the fish head. Panel 1 of Fig. 6 illustrates the general distribution of bone canals (BC) consisting of canals located in the bone structure of the fish head skeleton (Genten et al. 2010; Webb 1989; Lekander 1949). The BC system is typical of most bony fish (Genten et al. 2010) such as Arctic char. An important part of the cephalic lateral line system is accommodated in the bone canals (Genten et al. 2010).

Fish tissue sections with superimposed autoradiograms (in red) are shown in panels 2 to 4 of Fig. 6. Though the spatial resolution of tissue sections does not allow the direct observation of lines of bone canals, labeled areas observed correspond, at least partly, to the known locations of the lateral line bones (panel 3). Radiolabeled distribution observed just above the cranial bones is similar to the distribution of lines of bone canals seen in panel 3. Labeling is clearly restricted to narrow areas located between subdermic conjunctive tissues and cranial bones (outlined areas marked A in panels 2 and 3). Note that bone canal lines may feature many branches, which cannot be shown here since any detailed description of cephalic bone canals or of dermal bones distribution in Arctic char is available yet. Radioactivity is also detected between the vertebrae (outlined area B in panel 2), and the pattern may correspond to the location of bone canals. It is obviously not located close to the water-exposed skin of the fish.

A Brook trout (*Salvelinus fontinalis*) was used in the exposition experiment to free labeled ethanolamine, since the juvenile Arctic char was no more available at that time. Both species are physiologically close together, and this difference should not have influenced the distribution of labelled ethanolamine. The autoradiogram of the fish exposed to free

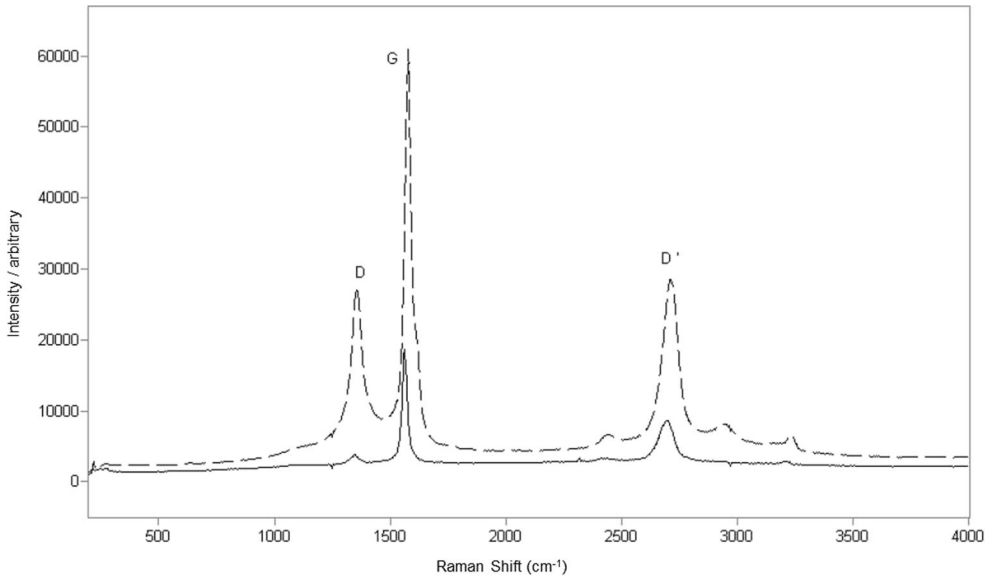

Fig. 3 Raman spectra of the raw (solid line) and carboxylated (dotted line) forms of the CNT1 with identification of D, G,and D' bands. Intensity units are arbitrary

labeled ethanolamine as a control shows a radioactivity pattern different from that exposed to amidated CNTs. The radioactivity is mainly located in olfactory bulb, gills, liver, and pyloric caeca and not in head bones (Figure S3). This observation suggests that biodistribution pattern observed in fish exposed to amidated f-CNTs is not an artifact due to free [^{14}C]-labeled ethanolamine or other amorphous carbon that could be produced during the process of preparing [14C]-labeled CNTs. Otherwise, the link between f-CNT and ethanolamine is a very strong C–N sigma bond attached to a ketone group (forming an amide group) and is not subject to a cleavage under low energy conditions (Kushuawa et al. 2013). Hydrolysis of amide is obtained only in hot alkali or strong acidic conditions as –NHR is a poor leaving group not reacting in water alone (Smith and March 2007). Hence, labeled [^{14}C]-ethanolamine is not expected to break off f-CNT after its reaction and cannot lead to erroneous labeling of soft tissues and bony structures where only [^{14}C]-ethanolamine would be present in the absence of f-CNT. Ethanolamine on itself is not expected to be bioaccumulated by living organisms as this small molecule is polar and labile.

A few papers reported only the distribution or toxic effects of raw or carboxylated CNTs on juvenile and adult fish (Maes et al. 2014; Felix et al. 2016; Campos-Garcia et al. 2016; Bjorkland et al. 2017). Various organ and cell pathologies were observed when fish were exposed to single-walled carbon nanotubes (SWCNT) for a 10-day period, including respiratory distress, gill irritation, and brain injury. Uptake of

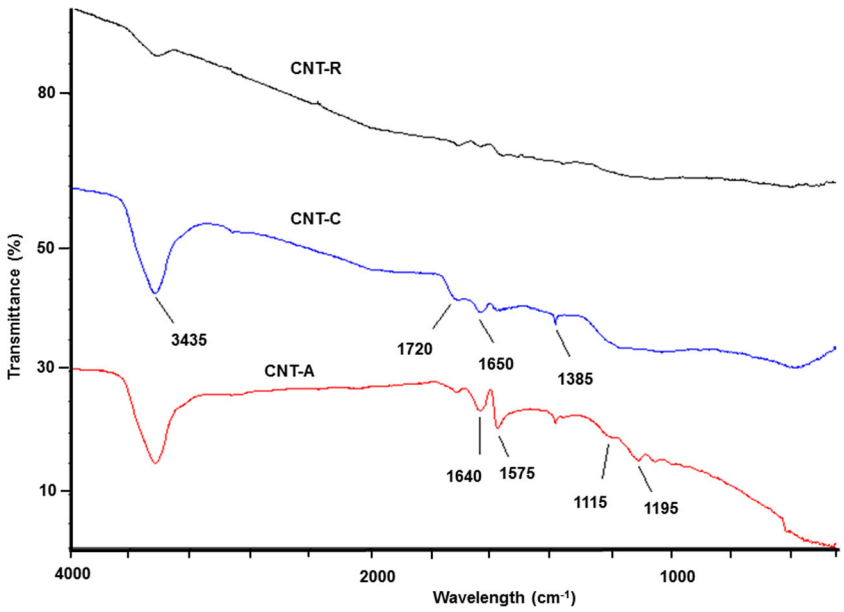

Fig. 4 FTIR spectra of the raw, carboxylated, and amidated forms of the CNT1

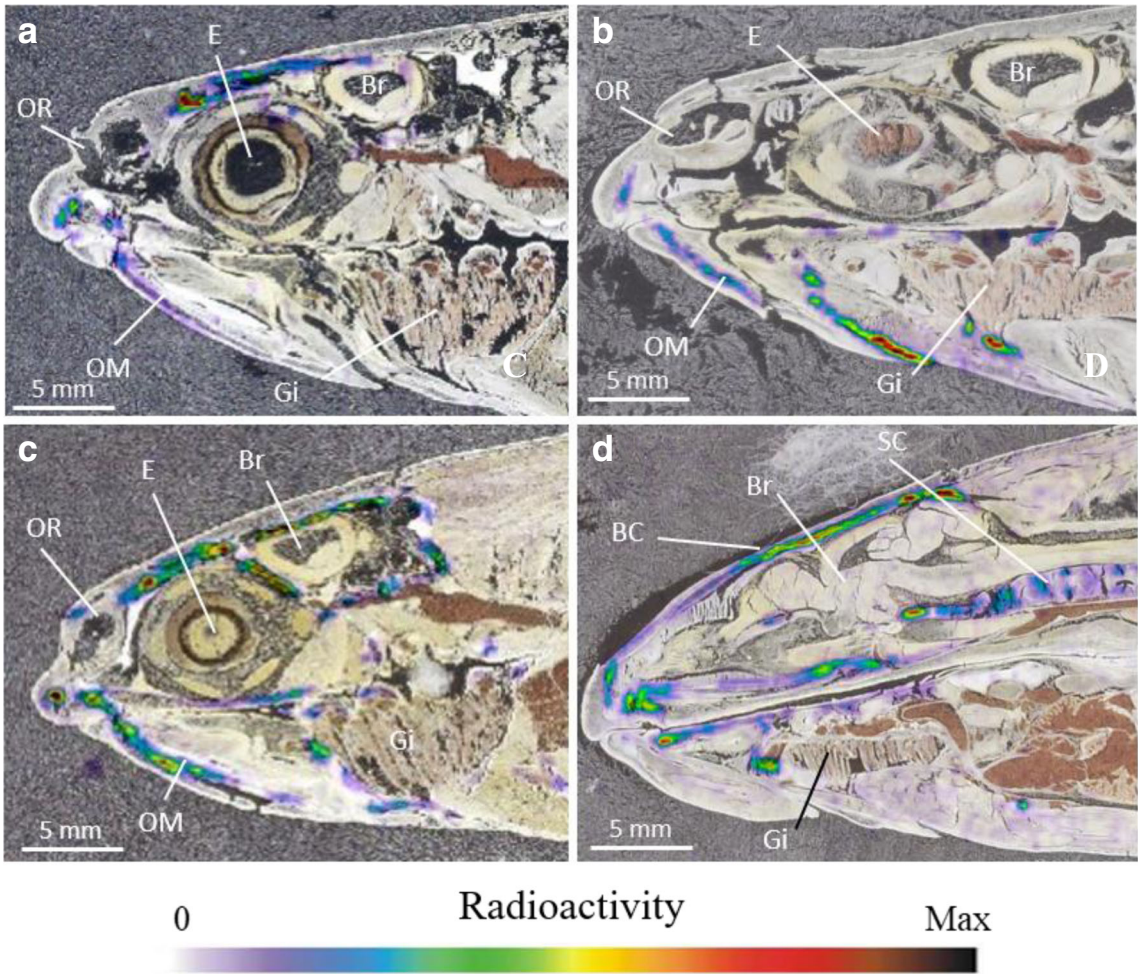

Fig. 5 Autoradiograms of the Arctic char exposed to functionalized [^{14}C]-f-CNT2 (**a** section # 26 and **b** section # 20) and to functionalized [^{14}C]- f-CNT1 (**c** section # 33 and **d** section #25). The sections are numbered from the first one (# 1) at the skin level to the last one on the opposite side of the fish. BC, bone canal; Br, brain; E, eye; Gi, gills; OM, operculo-mandibular canal; OR, olfactory bulb; SC, spinal cord

amine functionalized CNTs in whole plant or vegetables were studied (Zhai et al. 2015; Bjorkland et al. 2017). To our knowledge, reports on the distribution of amidated CNTs in fish bony tissues cannot be found in the literature. Yet, CNTs have excellent mechanical or chemical properties and promising uses in a wide range of bioengineering applications such as scaffolds for bone tissue engineering or stimulator of bone growth during osteoporosis by CNTs-bone interactions are expected (Bacakova et al. 2014).

Nanotubes and possible interactions with bone

A plausible explanation of radioactivity pattern accumulated in the bone canals is that CNTs might enter in the bone canals via the fluid-filled pores and be subsequently transported along vascular canals and cavities formed in bony tissue. Although the concentration of f-CNTs used in our experiment was relatively high (a few mg L^{-1}) and probably not at a realistic level from an environmental point of view, the uptake of CNTs via canal pores is most probably due to their very small size. The charged surface of functionalized CNTs could be responsible to the radioactivity clustered in bone canals of the Arctic char head (Fig. 5). Jang and Hwang (2018) reported that carboxylated f-CNTs could interact (e.g., adsorption) with metal ions such as lead (Pb^{2+}). Amidated CNTs prepared in our work (Fig. 7) have carboxyl, hydroxyl, and amide functionalities with negative (CNTs–COO^- ; $-O^-$, positive (CNTs–CO^-N^+HR) or neutral charges at pH 7. Electrostatic interactions can occur between both negative and positive CNT-A surface charges and positively (Ca^{2+})/negatively (PO_4^{3-}) charged moieties of bone material as illustrated by the CNTs-bone interactions model in Fig 7 (Saffar et al. 2009). Bone structure is composed of minerals, collagen, and water (Weiner and Wagner 1998). The main bone mineral component is calcium phosphate mineral also known as carbonated apatite (Saffar et al. 2009). Therefore, the carboxyl group attached to the f-CNT can lose proton (H^+) leading to a negative electrical charge distributed over both oxygen atoms. This electron density causes an unstable negative configuration tending to attract positively charged calcium ions of bones.

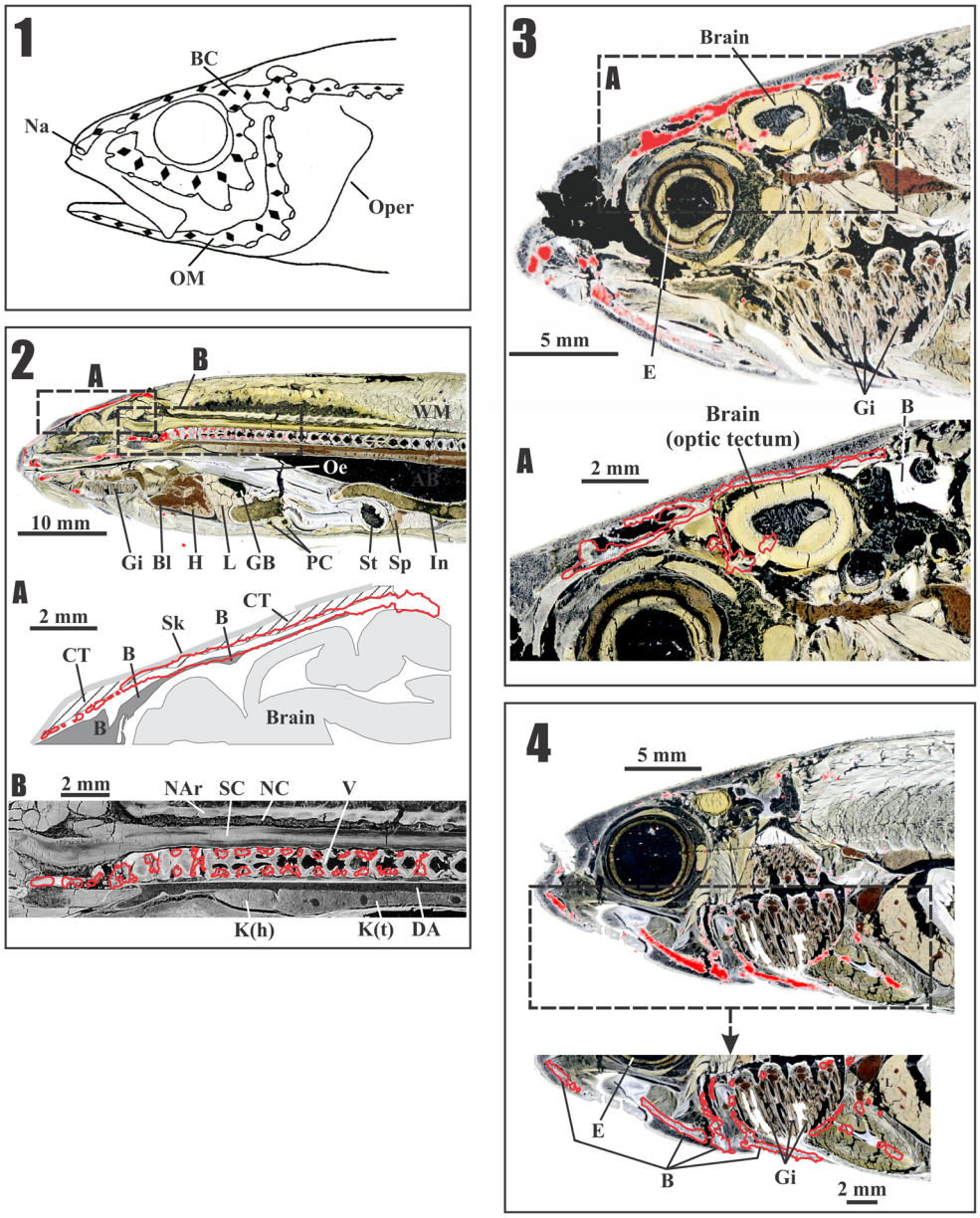

Fig. 6 Panel 1 shows bone channels system in a fish head adapted from Genten et al. (2010) and Webb (1989). Panel 2 shows tissue section with superposed autoradiogram (in red) of an Arctic char exposed to waterborne [^{14}C]-CNT1 for 3 h. Areas within dotted boxes labeled A and B are enlarged below. Panel 2A shows a drawing of the main anatomical structures superimposed with an outline (red) of the labeled areas. Panel 2B shows a black-and-white (b/w) enlargement of vertebral column superimposed with an outline (red) of the label areas. Panel 3 shows tissue section with superimposed autoradiogram (in red) of an Arctic char exposed to waterborne [^{14}C]-CNT2 for 3 h. Area within dotted 2 box 3A shows a b/w enlargement of cranium superimposed with an outline (red) of the label areas. Panel 4 shows tissue section with superposed autoradiogram (in red) from the same fish shown in panel 3 but a different section in the fish. Area within dotted box shows a b/w enlargement of the operculo-mandibular region superimposed with an outline (red) of the label areas. Only typical autoradiograms are shown but the same general distribution pattern of labeled CNTs was observed in all exposed fish. Bo, bone; BC, bone channels; Bl, blood; CT, connective tissue; DA, dorsal aorta; E, eye; GB, gall bladder; Gi, gills; H, heart; In, instestine; K(h), head kidney; K(t), trunk kidney; L, liver; Na, naris; Nar, neural arch; NC, neural canal; Oe, esophagus; OM, operculo-mandibular canal; Oper, operculum; OR, olfactory bulb; PC, pyloric caeca; SC, spinal cord; Sk, skin; Sp, spleen; St, stomach; V, vertebra; WM, white muscle

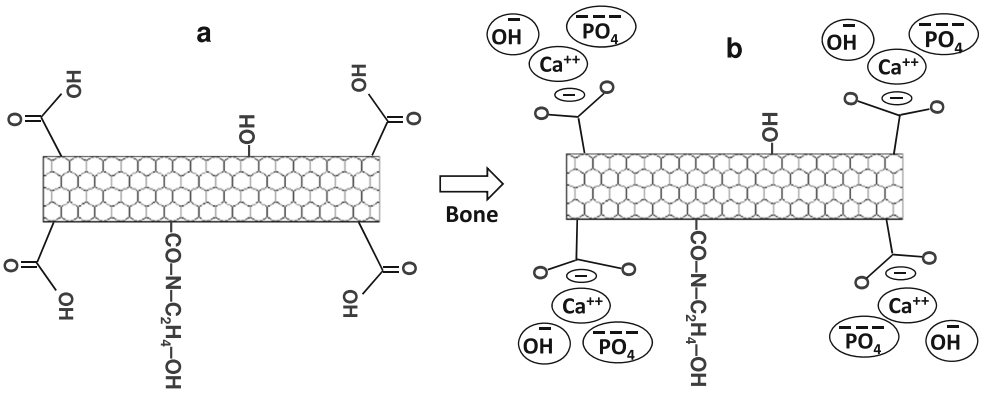

Fig. 7 Electrostatic interactions (attraction) model between f-CNTs carboxylate ions and bone calcium ions (adapted from Saffar et al. 2009)

As already reported, the functionalized-carbon nanotubes are promising materials for enhancing the bone physical stability because of their excellent ability to stimulate the bone tissue regeneration (Saffar et al. 2009).

Moreover, scanning electron microscopy (SEM) showed a strong degree of physical interactions between collagen matrix and carboxyl functionalized CNTs (Wang et al. 2015). Fibrous collagen, the organic phase of the bone, consists of three polypeptide chains of amino acids wound into a triple helix. This structure is conducive to hydrogen bonds and hydrophobic interactions with the f-CNTs. It was also found that the length of raw CNTs or the collagen does not significantly influence the hydrophobic interactions between the two systems (Gopalakrishnan et al. 2011). This result suggests that the partial charges or properties (e.g hydrophobicity) of surface functionalization CNTs (COO^-;O^-; N^+, C) could play a crucial role in interactions between bone matrix and f-CNTs. Figure 5 shows that the radioactivity pattern is more developed in bone canals of the fish head exposed to f-CNT1 (section C and D) comparatively to that exposed to [^{14}C]-f-CNT2 (section A and B). The size and interactions of CNTs with bones could be responsible for these differences. In addition, only the fish exposed to [^{14}C]-f-CNT1 shows a radioactivity pattern on the vertebral column with a low radiolabeling intensity (Figure S4). The large thickness and small size of CNT1 probably contributed to **a** greater accumulation of f-CNT1 in the head bone canals. This pattern suggests also that the [^{14}C]-f-CNT1 might interact more specifically with head bone canals. Indeed, more COOH groups are available on the surface of CNT1 compared to CNT2 for which amidation is more important (Table 1). Although the CNT2 radioactivity was twice the one of CNT1, a weak CNT2 interaction with bones could be explained by the lower radioactivity pattern observed in the fish exposed to [^{14}C]-CNT2. The positive charge of the CNT2 amide may be less available for electrostatic interactions with negative charges because of the carbonyl resonance which is important for the partial charge of the amide (Smith and March 2007). Further investigations of sorption interactions between different sizes or different hydroxylated CNTs and bones/collagens could allow a better understanding of the f-CNTs affinity for these materials.

Conclusion

Characterisation results show that the proposed method can be used with large and small raw CNTs, but results suggest that small CNT2 provides a better result with a higher -COOH substitution and a better specific activity of [^{14}C]. Using ethanolamine in this work as labeling strategy of raw CNTs appears as an adequate method to prepare functionalized [^{14}C]-CNTs in the objective of studying their behavior in environmental compartments. Results showed mainly an accumulation of amidated f-CNTs in the head of fish. This accumulation is attributed to the entry of [^{14}C]-CNTs in the bone canals via canal pores followed by possible interactions with the bone materials. Results suggest that more functionalized CNTs could induce a greater accumulation in the bone canals system.

Funding information This research work was funded by the Natural Sciences and Engineering Research Council of Canada and supported by the Canada Research Chair in Molecular Ecotoxicology (E.P).

Compliance with ethical standards

This research involved experiments on animals, Arctic char, due to the potential impact of f-CNTs on organisms in aquatic environment. This study was performed in strict accordance with Ethical Policy for Animal Experimentation (Publication No. C2-D34, Rev. 2012) approved by the Institutional Animal Care and Use Committee of the Université du Québec à Rimouski. This ethical policy is an application of the Canadian Council on Animal Care. Post-experimental cares of animals were provided including minimizing discomfort and the consequences of any disability resulting from the experiment.

Conflict of interest The authors declare that they have no conflict of interest (financial or non-financial).

References

Al-Sid-Cheikh M, Pelletier E, Rouleau C (2011) Synthesis and characterization of [110mAg]-nanoparticles with application to whole body autoradiography of aquatic organisms. Appl Radiat Isot 69: 1415–1142

Bacakova L, Kopova I, Stankova L, Liskova J, Vacik J, Lavrentiev V, Alexander Kromka A, Potocky S, Stranska D (2014) Bone cells in cultures on nanocarbonbased materials for potential bone tissue engineering: A review. Phys Status Solidi A 211:2688–2702

Bjorkland R, Tobias DA, Petersen EJ (2017) Increasing evidence indicates low bioaccumulation of carbon nanotubes. Environ Sci Nano 4:747–766

Campos-Garcia J, Martinez DS, Rezende KF, da Silva JR, Alves OL, Barbieri E (2016) Histopathological alterations in the gills of Nile tilapia exposed to carbofuran and multiwalled carbon nanotubes. Ecotoxicol Environ Saf 133:481–488

Chen P, Zhang HB, Lin GD, Hong Q, Tsai KR (1997) Gowth of carbon nanotubes by catalytic decomposition of CH_4 or CO on a Ni-MgO catalyst. Carbon 35:1495–1501

Cui HF, Vashist SK, Al-Rubeaan K, Luong JHT, Sheu FS (2010) Interfacing carbon nanotubes with living mammalian cells and cytotoxicity issues. Chem Res Toxicol 23:1131–1147

Datsyuk V, Kalyva M, Papagelis K, Parthenios J, Tasis D, Siokou A, Kallitsis I, Galiotis C (2008) Chemical oxidation of multi walled carbon nanotubes. Carbon 46:833–840

Deng X, Jia G, Wang H, Sun H, Wang X, Yang S, Wang T, Liu Y (2007) Translocation and fate of multi-walled carbon nanotubes in vivo. Carbon 45:1419–1424

Felix LC, Ede JD, Snell DA, Oliveira TM, Martinez-Rubi Y, Simard B, Luong JHT, Goss GG (2016) Physicochemical properties of functionalized carbon-based nanomaterials and their toxicity to fishes. Carbon 104:78–89

Forest GA, Alexander AJ (2007) A model for the dependence of carbon nanotube length on acid oxidation time. J Phys Chem C 111:10792–10798

Genten F, Terwinghe E, Danguy A (2010) Histologie illustrée du poisson. Quae edition, Paris, pp 379–402

Georgin, D., Czarny,B., Botquin, M., L'Hermite, M., Pinault, M., Bouchet-Fabre, B., Carriere, M., Poncy, J.L.; Chau, Q., Maximilien, R., Dive, V., Taran F., 2009. Preparation of the ^{14}C-labeled multi walled carbon nanotubes for the biodistribution investigation. J Am Chem Soc 131, 14658-14659.

Gopalakrishnan R, Balamurugan K, Singam ERA, Sundaraman S, Subramanian V (2011) Adsorption of collagen onto single walled carbon nanotubes: a molecular dynamics investigation. Phys Chem Chem Phys 13:13046–13057

Grandi, S., Magistis, A., Mustarelli, P., Quarterone, E., Tomasi, C., Meda, L., 2006. Synthesis and characterization of Si-O2-PEG hybrid materials. J Noncryst Sol. 352, 273-280.

Heller DA, Barone PW, Strano MS (2005) Sonication-induced changes in chiral distribution: A complication in the use of single-walled carbon nanotube fluorescence for determining species distribution. Carbon 43:651–673

Hou P, Liu C, Tong Y, Xu S, Liu M, Cheng H (2001) Purification of single-walled carbon nanotubes synthetized by the hydrogen arc-discharge method. J Mater Res 16:2526–2529

Iijima S (1991) Helical microtubules of graphitic carbon. Nature 354:56–58

Jackson P, Jacobsen NR, Baun A, Birkedal R, Kühnel D, Jensen KA, Vogel U, Wallin H (2013) Bioaccumulation and ecotoxicity of carbon nanotubes. Chem Cent J 7:154 A review

Jacoby A (2015) Global Markets and Technologies for Carbon Nanotubes. A BCC Research Nanotechnology Report, Report Code: NAN024F. http://www.bccresearch.com/market-research/nanotechnology/carbon-nantubes-global-markets-technologies-report-nan024f.html Visited 2019-03-15

Jang M-H, Hwang YS (2018) Effects of functionalized multi-walled carbon nanotubes on toxicity and bioaccumulation of lead in Daphnia magna. PLoS One 13(3):e0194935. https://doi.org/10.1371/journal.pone.0194935

Jia G, Wang H, Yan L, Wang X, Pei L, Yan T, Zhao Y, Guo X (2005) Cytotoxicity of carbon nanomaterials: single-wall nanotube, multi-wall nanotube, and fullerene. Environ Sci Technol 39:1378–1383

Kaempgen M, Lebert M, Haluska M, Nicoloso N, Roth S (2008) Sonochimical optimization of the conductivity of single-wall carbon nanotube networks. Adv Mater 20:616–620

Karimi M, Solati N, Amiri M, Mirshekari H, Mohamed E, Taheri M, Hashemkhani M, Saeidi A, Estiar MA, Kiani P, Ghasemi A, Basri SMM, Aref AR, Hamblin MR (2015) Carbon nanotubes part I: preparation of a novel and versatile drug-delivery vehicle. Expert Opin Drug Deliv 12:1071–1087

Kushuawa SKS, Ghoshal S, Rai AK, Singh S (2013) Carbon nanotubes as a novel drug delivery system for anticancer therapy: a review. Brazil. J Pharm Sci 49:629–643

Lekander B (1949) The sensory line system and the canal bones in the head of some Ostariophysi. Acta Zool 30:1–131

Maes HM, Stibany F, Giefers S, Daniels B, Deutschmann B, Werner Baumgartner W, Schäffer A (2014) Accumulation and distribution of Mmultiwalled carbon nanotubes in Zebrafish (Danio rerio). Environ Sci Technol 48:12256–12264

Mananghaya M (2015) Modeling of single-walled carbon nanotubes functionalized with carboxylic and amide groups towards its solubilization in water. J Mol Liq 212:592–596

Martınez MT, Callejas MA, Benito AM, Cochet M, Seeger T, Anson A, Schreiber J, Gordon C, Marhic C, Chauvet O, Fierro JLG, Maser WK (2003) Sensitivity of single wall carbon nanotubes to oxidative processing: structural modification, intercalation and functionalization. Carbon 41:2247–2256

Petersen EJ, Akkanen J, Kukkonen JVK, Weber WJ (2009) Biological uptake and depuration of carbon nanotubes by *Daphnia magna*. Environ Sci Technol 43:2969–2975

Petersen, E.J., Pinto, R.A., Zhang, L., Huang, Q., Landrum, P.F., Weber, Jr. W.J., 2011. Effects of polyethyleneimine-mediated functionalization of multi-walled carbon nanotubes on earthworm bioaccumulation and sorption by soils. Environ Sci Technol 45, 3718–3724.

Riddick JA, Bunger WB, Sakano TK (1986) Organic solvents - physical properties and methods of purification. Ed. A. Weissberger. John Wiley & Sons, New York, NY

Saffar KP, JamilPour N, and Rouhi G (2009) Carbon nanotubes in bone tissue engineering. Biomedical Engineering, Carlos Alexandre Barros de Mello (Ed.), 26, 477-498, InTechOpen.

Sajid MI, Jamshaid U, Jamshaid T, Zafar N, Fessi H, Elaissari A (2016) Carbon nanotubes from synthesis to *in vivo* biomedical applications. Int J Pharm 501:278–299

Smith MB, March J (2007) March's Advanced Organic Chemistry: Reactions, Mechanisms, and Structure (6th ed.), John Wiley & Sons, New York.

Sohn EK, Chung YS, Johari SA, Kim TG, Kim JK, Lee JH, Lee YH, Kang SW, Yu IJ (2015) Acute toxicity comparison of single-walled carbon nanotubes in various freshwater organisms. Biomed Res Int: 323090 7 pages

Solon EG (2007) Autoradiography: high-resolution molecular imaging in pharmaceutical discovery and development. Expert Opin Drug Discovery 2:503–514

Tasi D, Tagmatarchis N, Bianco A, Prato M (2006) Chemistry of carbon nanotubes. Chem Rev 106:1105–1136

Wang J., He C., Cheng N., Yang Q., Chen M., You L., Zhang Q. 2015. Bone marrow stem cells response to collagen/single-wall carbon nanotubes-COOHs nanocompositefFilms with transforming growth

factor Beta 1. J Nanosci Nanotechnol 15, 4844-4850, Bone Marrow Stem Cells Response to Collagen/Single-Wall Carbon Nanotubes-COOHs Nanocomposite Films with Transforming Growth Factor Beta 1.

Webb JF (1989) Gross morphology and evolution of the mecanoreceptive lateral-line system in teleost fishes. Brain Behav Evol 33:34–53

Weiner S, Wagner HD (1998) The material bone: structure-mechanical function relations. Annu Rev Mater Sci 28:271–298

Widiyarti G, Hanafi M, Isnijah S, Kardono LBS, Ngadiman E, Sundowo A (2009) Preparation of 2-aminoethylsulfonic acid. J Makara 13: 55–58

Wijnhoven SWP, Peijnenburg WJGM, Herberts CA, Hagens WI, Oomen AG, Heugens EHW, Roszek B, Bisschops J, Gosens I, Van De Meent D, Dekkers S, de Jong WH, van Zijverden M, Sips AJAM, Geertsma RE (2009) Nano-silver—A review of available data and knowledge gaps in human and environmental risk assessment. Nanotoxicology 3:109–138

Wu CS, Liao HT (2007) Study on the preparation and characterization of biodegradable polyactide/multi-walled carbon nanotubes nanocomposites. Polymer 48:4449–4458

Zardini HZ, Davarpanah M, Shanbedi M, Amiri A, Maghrebi M, Ebrahimi L (2014) Microbial toxicity of ethanolamines—Multiwalled carbon nanotubes. J Biomed Mater Res Part A 102A: 1774–1781

Zhai G, Gutowski SM, Walters KS, Yan B, Schnoor JL (2015) Charge, size, and cellular selectivity for multiwall carbon nanotubes by maize and soybean. Environ Sci Technol 49:7380–7390

Zhang L, Petersen EJ, Zhang W, Chen Y, Cabrera M, Huang Q (2012) Interactions of ^{14}C-labeled multi-walled carbon nanotubes with soil minerals in water. Environ Pollut 166:75–81

Zhang W, Zhang Z, Zhang Y (2011) The application of carbon nanotubes in target drug delivery systems for cancer therapies. Nanoscale Res Lett 6:555–577